Biosensors and Bioelectronics 98 (2017) 210–214

Contents lists available at ScienceDirect

Biosensors and Bioelectronics

journal homepage: www.elsevier.com/locate/bios

Pyrrolo-dC modified duplex DNA as a novel probe for the sensitive assay of base excision repair enzyme activity

Chang Yeol Lee[a], Ki Soo Park[b,*], Hyun Gyu Park[a,*]

[a] Department of Chemical and Biomolecular Engineering (BK 21+ program), KAIST, Daehak-ro 291, Yuseong-gu, Daejeon 305-338, Republic of Korea
[b] Department of Biological Engineering, College of Engineering, Konkuk University, Seoul 05029, Republic of Korea

ARTICLE INFO

Keywords:
Pyrrolo-dC
8-oxoguanine
Base excision repair
Formamidopyrimidine DNA glycosylase
Enzyme activity assay
Fluorescent biosensor

ABSTRACT

We develop a novel approach to determine formamidopyrimidine DNA glycosylase (Fpg) activity by taking advantage of the unique fluorescence property of pyrrolo-dC (PdC) positioned opposite to 8-oxoguanine (8-oxoG) in duplex DNA. In its initial state, PdC in duplex DNA undergoes the efficient stacking and collisional quenching interactions, showing the low fluorescence signal. In contrast, the presence of Fpg, which specifically removes 8-oxoG and incises resulting apurinic (AP) site, transforms duplex DNA into single-stranded (ss) DNAs. As a result, the intrinsic fluorescence signal of PdC in ssDNA is recovered to exhibit the significantly enhanced fluorescence signal. Based on this Fpg-dependent fluorescence response of PdC, we could reliably determine Fpg activity down to 1.25 U/ml with a linear response from 0 to 50 U/ml. In addition, the diagnostic capability of this strategy was successfully demonstrated by reliably assaying Fpg activity in human blood serum, showing its great potential in the practical applications.

1. Introduction

A variety of DNA damages induced by endogenous and exogenous factors have been known to threaten the genome integrity and cell viability. Among various DNA lesions in the cell, 8-oxoguanine (8-oxoG) generated by the persistent exposure to reactive oxygen species is the most common oxidative DNA damage product (Maehara et al., 2008; Obtułowicz et al., 2010). The 8-oxoG can form the mismatched base pair with adenine during DNA replication and thus cause the somatic mutation closely related to cancers (Agnihotri and Mishra, 2009; Bruner et al., 2000; Kuchino et al., 1987; Yadav and Mishra, 2014). The base excision repair (BER) pathway is recruited to prevent the potential adverse effects of damaged DNA (David and Williams, 1998; Fortini et al., 2003). Many enzymes such as N-glycosylases, endonucleases, end processing enzymes, polymerases, and ligases are involved in the BER pathway. Among them, N-glycosylases are of great importance due to their role in the initiation of BER pathway. In addition, the BER capabilities of these enzymes are known to serve as an indicator for assessing the risk of cancers (David et al., 2007). The representative example of N-glycosylases is 8-oxoG DNA glycosylases possessing both N-glycosylase and AP-lyase activities, which function in the BER pathway by releasing the damaged purines (i.e. 8-oxoG) from duplex DNA, generating apurinic (AP) sites, and cleaving them to produce a nucleobase gap or 5'-phosphate and 3'-phospho-α,β-unsaturated aldehyde (Liu et al., 2013; McWilliams et al., 2014).

Owing to biological and clinical significance of 8-oxoG DNA glycosylases, a lot of methods for determining their repair activities have been developed, such as HPLC (Ravanat et al., 1998; Rebelo et al., 2004), comet assay (Park et al., 2009), gel electrophoresis with radioactive labeling (Gackowski et al., 2003; Lin et al., 2000), western blot with immunohistochemistry (Gao et al., 2013; Xu et al., 2013), fluorescence-based methods (Liu et al., 2012; Mirbahai et al., 2010; Sauvaigo et al., 2004), and colorimetric methods (Liu et al., 2013; Yuan et al., 2015). Among these, optical methods are the most promising in the sensitivity, however, they have some drawbacks including the requirement of specialized equipment, complicated procedures, and expensive assay materials (Liu et al., 2012, 2013; Mirbahai et al., 2010; Sauvaigo et al., 2004; Yuan et al., 2015). Therefore, there still exists a great need for the development of novel assay systems which permit high sensitivity, efficient operability, and cost-effectiveness.

Toward this goal, we have developed a novel optical system for the sensitive determination of 8-oxoG DNA glycosylase by utilizing a unique fluorescence property of pyrrolo-dC (PdC). PdC, a fluorescent analog of cytosine (C) nucleobase that selectively hybridizes with the guanine, has the hybridization-dependent fluorescence property: when it is incorporated into duplex DNA, its fluorescence intensity is significantly quenched, while the dissociation of duplex DNA into single-stranded (ss) DNAs enhances the fluorescence of PdC by

* Corresponding authors.
E-mail addresses: kskonkuk@gmail.com (K.S. Park), hgpark@kaist.ac.kr (H.G. Park).

http://dx.doi.org/10.1016/j.bios.2017.06.052
Received 14 April 2017; Received in revised form 7 June 2017; Accepted 25 June 2017
Available online 27 June 2017
0956-5663/

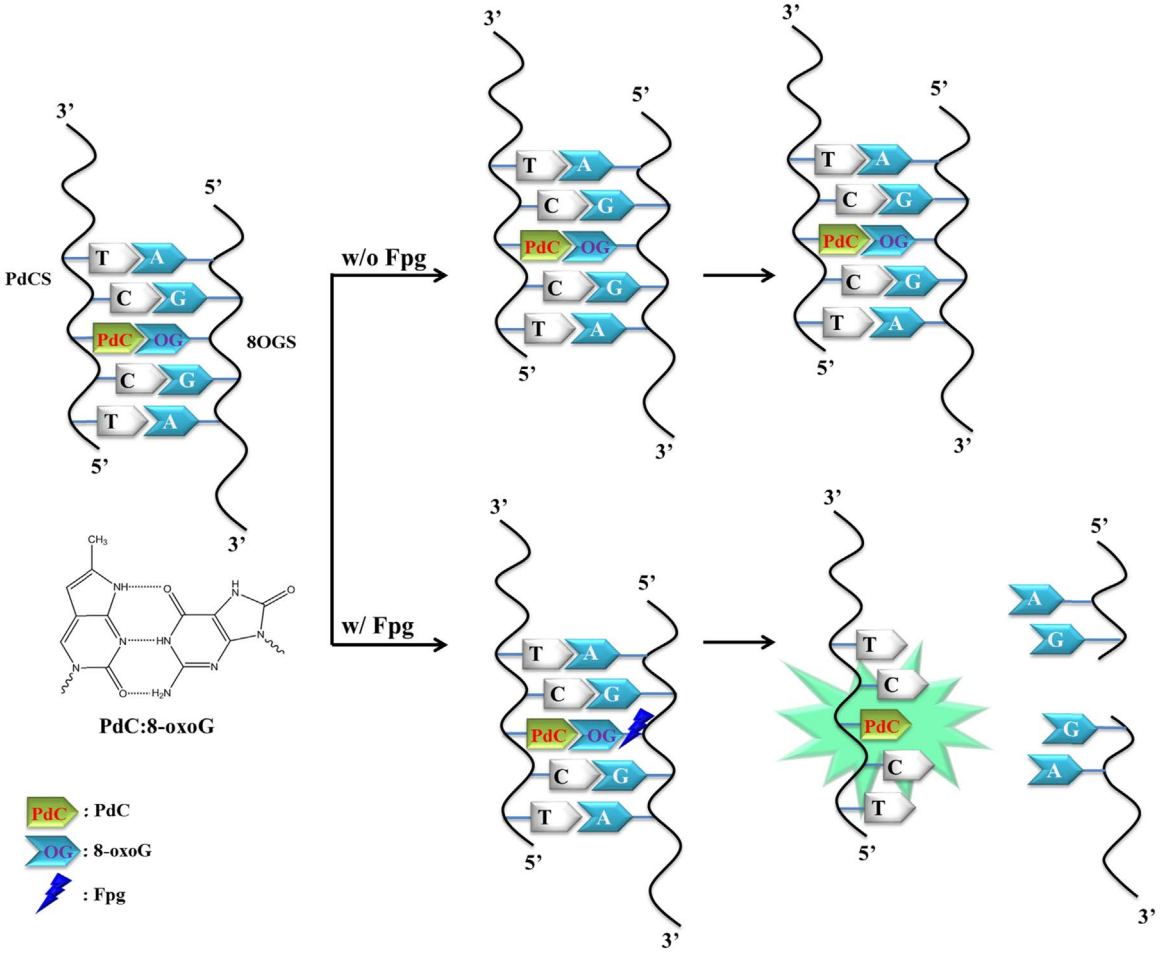

Scheme 1. Schematic illustration of the Fpg activity assay utilizing the duplex DNA probe having a base pair of 8-oxoG:PdC.

reducing the stacking and collisional quenching interactions (Li et al., 2010; Liu and Martin, 2002; Park et al., 2012; Wilhelmsson, 2010). We believed that this unique fluorescence property of PdC would serve as a new sensing platform for enzymatic activities without the requirement of the expensive modification with fluorophore and quencher. Herein, we have selected formamidopyrimidine DNA glycosylase (Fpg) as a target 8-oxoG DNA glycosylase and rationally designed the duplex DNA to form a 8-oxoG:PdC base pair such that its fluorescence signal becomes dependent on the Fpg-catalyzed cleavage reaction that induces the transformation of the duplex DNA into ssDNAs. With this novel system, we successfully determined the Fpg activity with the high sensitivity and selectivity and verified the clinical capability by reliably detecting Fpg activity in human blood serum.

2. Materials and methods

2.1. Materials

All DNA strands used in the study were synthesized by Genotech Co. (Daejeon, South Korea) and purified by HPLC, except for 8OGP-H1 and 8OGP-H2 (purified by desalting). The sequences of DNA oligonucleotides are listed in Table S1. Formamidopyrimidine DNA glycosylase (Fpg), uracil DNA glycosylase (UDG), exonuclease I (Exo I), exonuclease III (Exo III), ribonuclease H (RNase H), Hind III, *Eco*RI, Nt.AlwI, shrimp alkaline phosphatase (ALP), *E.coli* DNA ligase, and bovine serum albumin (BSA) were purchased from New England Biolabs Inc. (Beverly, MA, USA). Human serum was purchased from Sigma-Aldrich. All other chemicals were of analytical grade and used without further purification. Ultrapure DNase/RNase-free distilled water purchased from Bioneer® (Daejeon, Korea) was used throughout all the experiments.

2.2. Fpg activity detection procedure

5 μl of 8OGS (5 μM), 5 μl of PdCS (5 μM), 0.5 μl of BSA (10 mg/ml) and 5 μl of 10X NEBuffer 2 (10 mM Tris-HCl, 50 mM NaCl, 10 mM $MgCl_2$, 1 mM DTT, pH 7.9 at 1X concentration) were mixed to prepare the reaction mixtures of 45 μl. The reaction mixtures were heated at 85 °C for 5 min, cooled slowly to 37 °C (0.1 °C/s), and incubated at 37 °C for 20 min to form a duplex substrate (8OGS/PdCS duplex). After the incubation, 5 μl of Fpg at varying concentrations was added to the reaction mixtures. The enzymatic reaction was conducted at 37 °C for 60 min, followed by the fluorescence measurement at room temperature. The fluorescence emission spectra were recorded in the range from 400 to 600 nm at an excitation wavelength of 350 nm.

2.3. Gel electrophoresis analysis of enzymatic reaction products

The enzymatic reaction products were resolved on 15% polyacrylamide gel using 1X TBE as a running buffer at a constant voltage of 100 V for 75 min. After SYBR gold (Invitrogen, CA, USA) staining, gels were visualized using an UV transilluminator (Park et al., 2015).

2.4. Preparation and analysis of human serum samples

In order to minimize the interference from human serum proteins, a solution of human serum diluted 10 times with NEBuffer 2 was loaded into a centrifugal filter device (MWCO = 100,000 Da, Millipore).

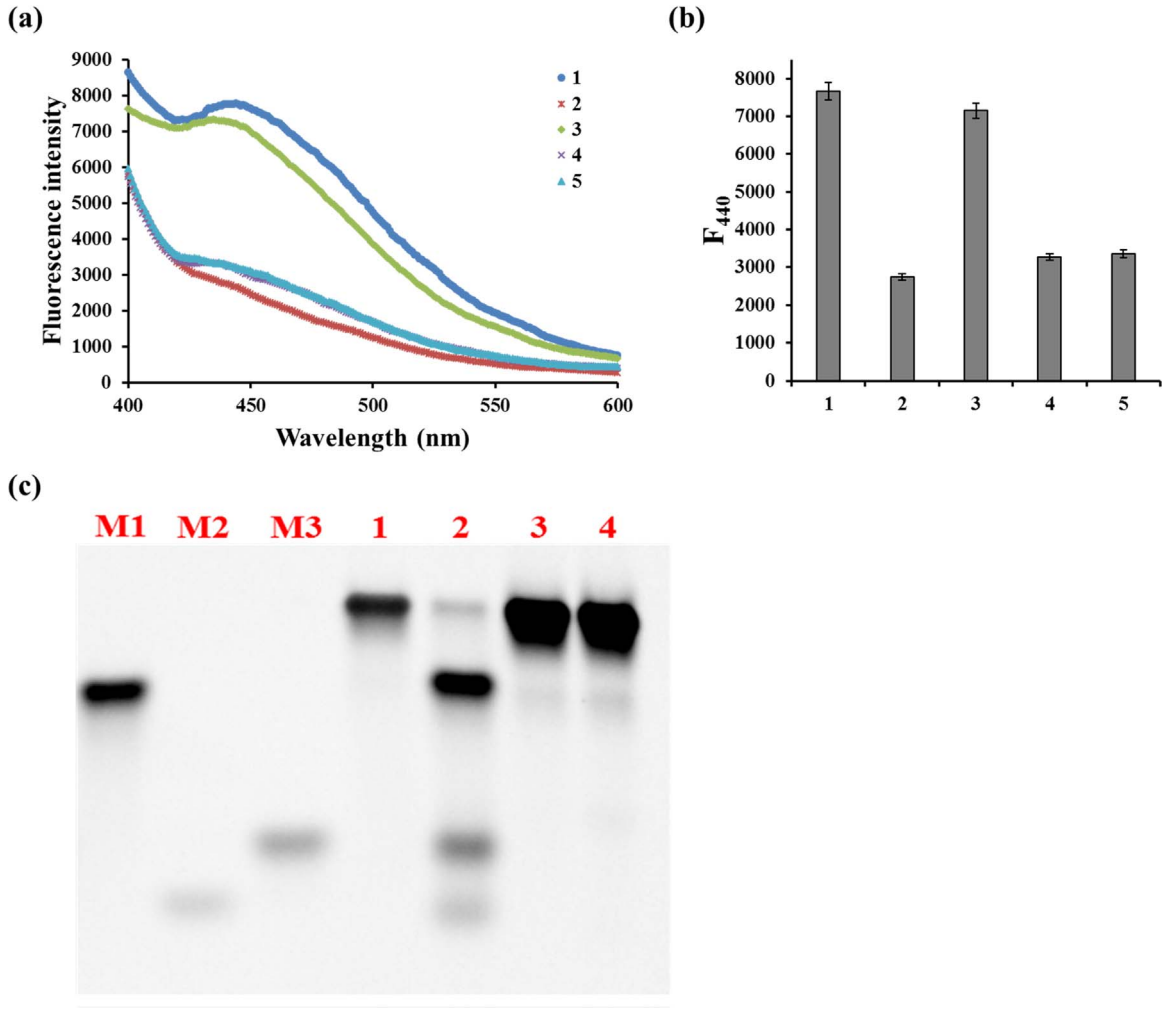

Fig. 1. Feasibility of the Fpg activity assay. Fluorescence emission spectra (a) and intensities at 440 nm (b) from PdC in the different samples (1: PdCS, 2: 8OGS/PdCS duplex without Fpg, 3: 8OGS/PdCS duplex with Fpg, 4: GS/PdCS duplex without Fpg, 5: GS/PdCS duplex with Fpg). (c) Polyacrylamide gel electrophoresis image of resulting products after treatment with Fpg (1: 8OGS/PdCS duplex without Fpg, 2: 8OGS/PdCS duplex with Fpg, 3: GS/PdCS duplex without Fpg, 4: GS/PdCS duplex with Fpg). Lanes M1, M2, and M3 show the size markers for PdCS, 8OGS-H1, and 8OGS-H2, respectively. The final concentrations of PdCS, 8OGS/PdCS duplex, GS/PdCS duplex, and Fpg are 500 nM, 500 nM, 500 nM, and 50 U/ml, respectively.

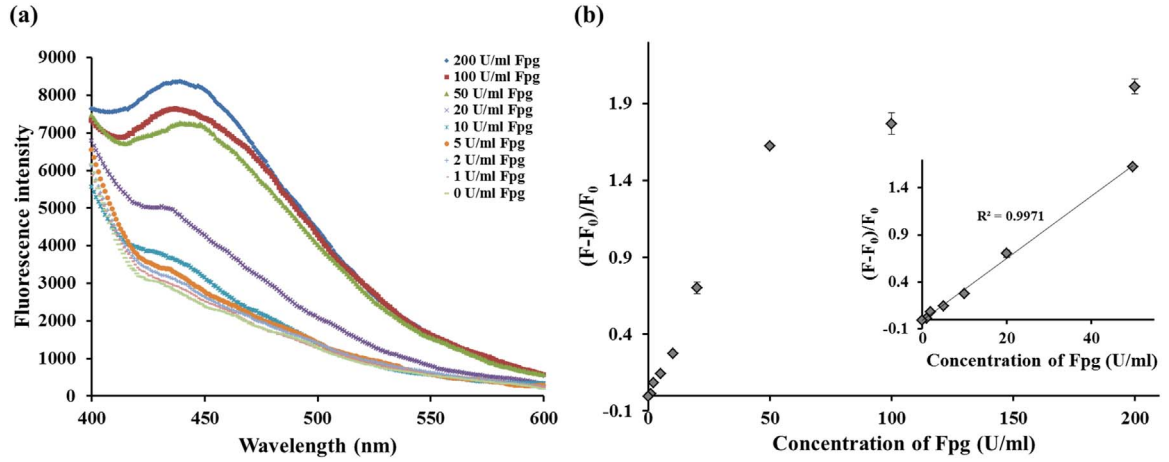

Fig. 2. Sensitivity of the Fpg activity assay. (a) Fluorescence emission spectra from PdC after treatment with Fpg at varying concentrations. (b) The degrees of signal enhancement in the presence of Fpg at varying concentrations. The degree of signal enhancement is defined as $(F\text{-}F_0)/F_0$, where F_0 and F are the fluorescence intensities at 440 nm from PdC in the absence and presence of Fpg, respectively. Inset: Linear range between $(F\text{-}F_0)/F_0$ and the Fpg concentration (0–50 U/ml). The final concentration of 8OGS/PdCS duplex is 500 nM.

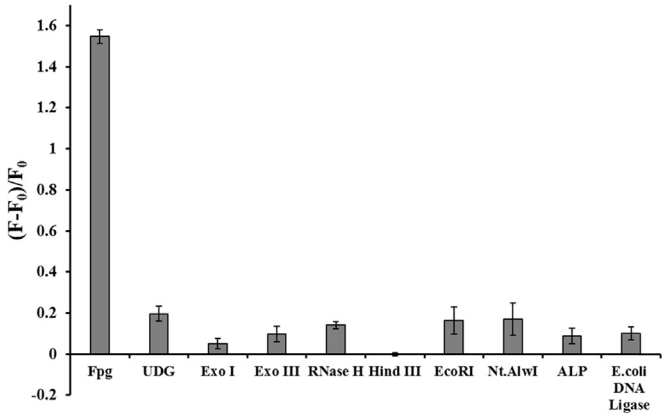

Fig. 3. Specificity of the Fpg activity assay. Fluorescence responses after treatment with Fpg (50 U/ml) and other enzymes (150 U/ml). The degree of signal enhancement is defined as $(F-F_0)/F_0$, where F_0 and F are the fluorescence intensities at 440 nm from PdC in the absence and presence of the enzyme, respectively. The final concentration of 8OGS/PdCS duplex is 500 nM.

Table 1
Determination of Fpg activity in diluted human serum.[a]

Added Fpg (U/ml)	Measured Fpg (U/ml)[b]	SD[c]	CV[d] (%)	Recovery[e] (%)
15	14.9	0.69	4.63	99.3
30	30.8	0.30	0.96	102.6
45	44.1	1.46	3.30	98.0

[a] To determine Fpg activity, a calibration curve was first created by using standards having known Fpg activities in human serum (Fig. S3). Based on this calibration curve, the fluorescence intensities from the unknown samples were used to determine Fpg activity present in human serum.
[b] Mean of three measurements.
[c] Standard deviation of three measurements.
[d] Coefficient of variation = SD/mean × 100.
[e] Measured value/added value × 100.

The sample was then subjected to centrifugation at 6000*g*-force for 20 min (Li et al., 2012; Park et al., 2014b; Zong et al., 2017). Finally, Fpg was spiked into the filtered human serum at different concentrations. Each sample was then analyzed by following the same procedure to determine Fpg activity as described above.

2.5. Instrumentation

Fluorescence intensities were measured using a Tecan Infinite M200 pro microplate reader (Mnnedorf, Switzerland) and black, 384-well Greiner Bio-One microplates (ref: 781077, Courtaboeuf, France) (Park et al., 2014a; Park and Park, 2015). The image of gel electrophoresis was obtained by using Gel Doc EZ Imager (Bio-rad, Hercules, USA).

3. Results and discussion

3.1. Overall detection principle

The basic principle of the new strategy to determine the Fpg activity is depicted in Scheme 1. This strategy utilizes the rationally designed duplex DNA probe composed of 8-oxoG-incorporated strand (8OGS) and PdC-incorporated strand (PdCS). Taking into account our previous finding that PdC flanked by C induced the highest fluorescence difference between ss and double-stranded forms of DNA, C was located on both flanks of PdC to maximize the target-induced fluorescence change (Park et al., 2012). In addition, the duplex DNA probe is designed to contain 3' ss-overhang sequences for both strands such that it is resistant to the exonuclease III-catalyzed digestion and becomes selective only towards Fpg (Lin et al., 2014). In the absence of Fpg, the 8-oxoG:PdC base pair in the duplex DNA remains intact and its original structure is retained. In this case, PdC in the duplex DNA not only experiences the efficient stacking with neighboring nucleobases, which leads to the electron transfer quenching of PdC, but also contacts with neighboring nucleobases to induce the collisional quenching through which PdC at its excited state becomes deactivated to the ground state without the fluorescence emission (Hardman and Thompson, 2006; Kimura et al., 2007; Martí et al., 2006; Rachofsky et al., 2001; Zhang et al., 2011). As a result, PdC exhibits the quite reduced fluorescence signal. On the other hand, the presence of Fpg cleaves the N-glycosylic bond between deoxyribose and damaged base, 8-oxoG, and incises the resulting AP site, which decreases the melting temperature of duplex DNA probe and thereby releases 8OGS far away from PdCS. Accordingly, the interactions that induce the fluorescence quenching of PdC are significantly diminished, consequently leading to the significant fluorescence enhancement of PdC.

3.2. Feasibility of the strategy

The optimal conditions for the efficient analysis of Fpg activity were first explored. The results of the experiments in which the concentration ratio of 8OGS to PdCS, Fpg reaction time, pH, and salt concentrations were varied, show that 1:1 ratio of 8OGS to PdCS, 60 min of Fpg reaction, 7.9 of pH, 10 mM of Mg^{2+}, and 50 mM of Na^{+} are ideal for the efficient assay of Fpg activity (Fig. S1). Under these conditions, fluorescence measurements were then performed to verify the feasibility of the developed system. As envisioned, in the absence of Fpg, the weak fluorescence was exhibited (2, Fig. 1(a) and (b)). In contrast, the significant enhancement of fluorescence signal at 440 nm, a peak emission wavelength of PdC, was observed when 8OGS/PdCS duplex was treated with Fpg. The enhanced fluorescence signal was comparable to that from PdCS (1 and 3, Fig. 1(a) and (b)). To demonstrate that the high fluorescence enhancement of PdC exclusively originates from the catalytic activity of Fpg that specifically recognizes 8-oxoG in the duplex DNA, GS in which the 8-oxoG residue in 8OGS is replaced with a guanine residue, was designed to form a duplex DNA with PdCS (GS/PdCS duplex), which was treated with Fpg (Table S1). Importantly, the presence of Fpg did not enhance the quenched fluorescence signal, which was comparable to those from 8OGS/PdCS and GS/PdCS duplexes in the absence of Fpg (2, 4, and 5, Fig. 1(a) and (b)). Overall, these results confirm that the fluorescent enhancement of PdC is induced by the Fpg-catalyzed reaction specific to 8-oxoG-incorporated duplex DNA probe.

The polyacrylamide gel electrophoresis (PAGE) analysis of products obtained after Fpg-catalyzed reactions was also performed to support the fluorescence results in Fig. 1(a) and (b). As illustrated in Fig. 1(c), in the absence of Fpg, a single intense band was observed in both lane 1 and lane 3, which implies the maintenance of duplex DNA (8OGS/PdCS in lane 1 and GS/PdCS in lane 3). However, the presence of Fpg dissociated 8OGS/PdCS duplex and the band corresponding to 8OGS/PdCS duplex disappeared. Instead, three bands appeared at the lower position, which correspond to the reaction product composed of PdCS, 8OGS-H1, and 8OGS-H2 (Lanes M1, M2, M3, and 2, Fig. 1(c)). Importantly, GS/PdCS duplex treated with Fpg was not dissociated, as evidenced by a single intense band at the same position with that of lane 3 (Lane 4, Fig. 1(c)). The results from PAGE analysis are consistent with the fluorescence spectral data, ensuring the feasibility of the proposed approach.

3.3. Sensitivity and selectivity of the strategy

The detection sensitivity of this sensing strategy was then determined by measuring the fluorescence intensities at 440 nm as a function of target Fpg concentration (Fig. 2). The results show that fluorescence intensities increase with increasing concentrations of Fpg up to 50 U/ml, but reach a plateau at concentrations higher than 50 U/

ml (Fig. 2). An excellent linear relationship (R^2 = 0.9971) exists in the range of 0–50 U/ml and the limit of detection (LOD) (3σ/slope) is ca. 1.25 U/ml, a value that is comparable to that of the recently reported method to determine the Fpg activity (Fig. 2(b)) (McWilliams et al., 2014; Sauvaigo et al., 2004; Wu et al., 2015). In addition, its reproducibility and stability were examined by calculating the relative standard deviations (RSDs, *n*=5) and measuring the fluorescence intensities for 12 h, respectively. The RSDs at four different concentrations of Fpg (0 U/ml, 10 U/ml, 20 U/ml, and 50 U/ml) were 1.02%, 1.29%, 2.32%, and 0.46%, respectively, which are less than 10%, showing the excellent reproducibility (Mei et al., 2015). The fluorescence change induced by the Fpg activity was stable for 12 h, indicating that this strategy is highly reliable and stable (Fig. S2).

To investigate the specificity of the new detection system towards Fpg, the abilities of other DNA glycosylase (UDG), nucleases (Exo I, Exo III, RNase H, Hind III, *Eco*RI, and Nt.AlwI), end processing enzyme (ALP), and ligase (*E.coli* DNA ligase) to induce the high fluorescence enhancement were examined and compared with that of Fpg. As shown in Fig. 3, the significant fluorescence enhancement was observed only when Fpg was applied. On the contrary, the other enzymes resulted in the negligible signal enhancement even though they were present at higher concentration than that of Fpg. In particular, the negligible signal enhancement was exhibited in the presence of Exo III because 8OGS/PdCS duplex was designed to have 3' protruding termini to avoid the degradation by Exo III. These results demonstrate that the developed strategy is highly selective toward Fpg and the fluorescence enhancement of PdC exclusively arises from the Fpg-promoted catalytic reaction.

3.4. Real sample analysis

Finally, the practical applicability of the new assay system was verified by determining Fpg activity present in human serum which generally contains proteins, hormones, glucose, and other biological interferences (Park et al., 2013). The serum samples spiked with Fpg were analyzed and the concentrations of Fpg in serum samples were determined from the standard curve (Table 1 and Fig. S3). As shown in Table 1, the Fpg activities in diluted human serum (1%) could be successfully assayed with excellent reproducibility and precision, as evidenced by the coefficients of variation (< 5%) and recovery rates (98.0–102.6%) (Park et al., 2014b). These observations indicate that the present assay has the capability to reliably determine the activities of Fpg in biological samples.

4. Conclusion

In this study, we have developed a novel fluorescent strategy for the sensitive assay of Fpg activity by rationally designing the duplex DNA probe to form the 8-oxoG:PdC base pair. Fpg-catalyzed reaction involving the removal of 8-oxoG and incision of resulting AP site, dissociates the duplex DNA into ssDNAs and diminishes the stacking interaction and collisional quenching, consequently leading to the significant fluorescence enhancement of PdC. With this novel approach that does not require the expensive modification of fluorophore and quencher, Fpg activity was detected down to 1.25 U/ml, and its diagnostic capability was demonstrated by reliably assaying the Fpg activity in human blood serum. In the follow-up experiment, a large cohort of cancer patients will be tested to evaluate the practical applicability of the developed system. To the best of our knowledge, this is the first report to analyze the activity of BER enzyme by exploiting the fluorescent nucleobase analog positioned opposite to the damaged nucleobase. Finally, we expect that this simple sensing strategy can be expanded to assay the other BER enzyme activities by rationally designing the DNA probes to be specific for the target BER enzymes.

Acknowledgements

This work was supported by the Mid-career Researcher Support Program through the National Research Foundation (NRF) funded by the Ministry of Science, ICT & Future Planning (MSIP) of Korea (No. 2015R1A2A1A01005393) and by the Center for BioNano Health-Guard funded by the MSIP of Korea as Global Frontier Project (Grant H-GUARD_2013M3A6B2078964). Financial support was also provided by the NRF grant funded by the MSIP of Korea (No. 2017R1C1B5017724).

Appendix A. Supplementary material

Supplementary data associated with this article can be found in the online version at doi:10.1016/j.bios.2017.06.052.

References

Agnihotri, N., Mishra, P., 2009. J. Phys. Chem. B 113, 3129–3138.
Bruner, S.D., Norman, D.P., Verdine, G.L., 2000. Nature 403, 859–866.
David, S.S., O'Shea, V.L., Kundu, S., 2007. Nature 447, 941–950.
David, S.S., Williams, S.D., 1998. Chem. Rev. 98, 1221–1262.
Fortini, P., Pascucci, B., Parlanti, E., D'errico, M., Simonelli, V., Dogliotti, E., 2003. Biochimie 85, 1053–1071.
Gackowski, D., Speina, E., Zielinska, M., Kowalewski, J., Rozalski, R., Siomek, A., Paciorek, T., Tudek, B., Olinski, R., 2003. Cancer Res. 63, 4899–4902.
Gao, D., Hu, J., Zhang, X., Gao, C., Hong, J., 2013. Cancer Biother. Radiopharm. 28, 433–440.
Hardman, S.J., Thompson, K.C., 2006. Biochemistry 45, 9145–9155.
Kimura, T., Kawai, K., Fujitsuka, M., Majima, T., 2007. Tetrahedron 63, 3585–3590.
Kuchino, Y., Mori, F., Kasai, H., Inoue, H., Iwai, S., Miura, K., Ohtsuka, E., Nishimura, S., 1987. Nature 327, 77–79.
Li, T., Fu, R., Park, H.G., 2010. Chem. Commun. 46, 3271–3273.
Li, J., Zhong, X., Zhang, H., Le, X.C., Zhu, J.-J., 2012. Anal. Chem. 84, 5170–5174.
Lin, L.H., Cao, S., Yu, L., Cui, J., Hamilton, W.J., Liu, P.K., 2000. J. Neurochem. 74, 1098–1105.
Lin, C., Wu, Y., Luo, F., Chen, D., Chen, X., 2014. Biosens. Bioelectron. 59, 365–369.
Liu, C., Martin, C.T., 2002. J. Biol. Chem. 277, 2725–2731.
Liu, S.-C., Wu, H.-W., Jiang, J.-H., Shen, G.-L., Yu, R.-Q., 2013. Anal. Methods 5, 164–168.
Liu, B., Yang, X.-H., Wang, K.-M., Tan, W.-H., 2012. Chem. J. Chin. Univ. 33, 486–491.
Maehara, Y., Egashira, A., Oki, E., Kakeji, Y., Tsuzuki, T., 2008. Cancer Sci. 99, 451–458.
Martí, A.A., Jockusch, S., Li, Z., Ju, J., Turro, N.J., 2006. Nucleic Acids Res. 34, e50.
McWilliams, M.A., Anka, F.H., Balkus, K.J., Slinker, J.D., 2014. Biosens. Bioelectron. 54, 541–546.
Mei, M., Huang, X., Liao, K., Yuan, D., 2015. Anal. Chim. Acta 860, 29–36.
Mirbahai, L., Kershaw, R.M., Green, R.M., Hayden, R.E., Meldrum, R.A., Hodges, N.J., 2010. DNA Repair 9, 144–152.
Obtułowicz, T., Swoboda, M., Speina, E., Gackowski, D., Rozalski, R., Siomek, A., Janik, J., Janowska, B., Cieśla, J.M., Jawien, A., 2010. Mutagenesis 25, 463–471.
Park, K.S., Kim, M.I., Woo, M.-A., Park, H.G., 2013. Biosens. Bioelectron. 45, 65–69.
Park, K.S., Lee, J.Y., Park, H.G., 2012. Chem. Commun. 48, 4549–4551.
Park, K.S., Lee, C.Y., Park, H.G., 2014a. Analyst 139, 4691–4695.
Park, K.S., Lee, C.Y., Park, H.G., 2015. Chem. Commun. 51, 9942–9945.
Park, J.-H., Mangal, D., Frey, A.J., Harvey, R.G., Blair, I.A., Penning, T.M., 2009. J. Biol. Chem. 284, 29725–29734.
Park, K.S., Oh, S.S., Soh, H.T., Park, H.G., 2014b. Nanoscale 6, 9977–9982.
Park, K.S., Park, H.G., 2015. Biosens. Bioelectron. 64, 618–624.
Rachofsky, E.L., Osman, R., Ross, J.A., 2001. Biochemistry 40, 946–956.
Ravanat, J.-L., Gremaud, E., Markovic, J., Turesky, R.J., 1998. Anal. Biochem. 260, 30–37.
Rebelo, I.A., Piedade, J.A.P., Oliveira-Brett, A.M., 2004. Talanta 63, 323–331.
Sauvaigo, S., Guerniou, V., Rapin, D., Gasparutto, D., Caillat, S., Favier, A., 2004. Anal. Biochem. 333, 182–192.
Wilhelmsson, L.M., 2010. Q. Rev. Biophys. 43, 159–183.
Wu, Y., Yang, X., Zhang, B., Guo, L.-H., 2015. Biosens. Bioelectron. 69, 235–240.
Xu, X., Wang, Y., Guo, W., Zhou, Y., Lv, C., Chen, X., Liu, K., 2013. J. Ovarian Res. 6, 74.
Yadav, A., Mishra, P., 2014. Chem. Phys. Lett. 592, 232–237.
Yuan, F., Zhao, H., Liu, M., Quan, X., 2015. Biosens. Bioelectron. 68, 7–13.
Zhang, H., Wang, M., Gao, Q., Qi, H., Zhang, C., 2011. Talanta 84, 771–776.
Zong, C., Wang, M., Li, B., Liu, X., Zhao, W., Zhang, Q., Liang, A., Yu, Y., 2017. RSC Adv. 7, 26559–26565.